Flip and Flop: A Molecular Determinant for AMPA Receptor Channel Opening[†]

Weimin Pei, Zhen Huang, Congzhou Wang, Yan Han, Jae Seon Park, and Li Niu*

Department of Chemistry, Center for Neuroscience Research, University at Albany, State University of New York, Albany, New York 12222

Received August 23, 2008; Revised Manuscript Received March 9, 2009

ABSTRACT: Alternative splicing in the extracellular ligand binding domain of the AMPA receptors generates two variants, i.e., flip and flop. The flop variant of the GluR2 AMPA receptor is known to desensitize faster than the flip counterpart, whereas the GluR1 flip and flop variants exhibit the same rate of desensitization. However, whether the alternative splicing affects the channel opening kinetic properties of these receptors is unknown. Using a laser-pulse photolysis technique, we have characterized the channel opening kinetic mechanism for the flip and flop channels of GluR1 and GluR2, respectively. We find that the flop variant of GluR2 opens the channel, following the binding of glutamate, with the same rate as the flip channel, but closes its channel more rapidly. The difference in the kinetic properties between the two receptor isoforms can be described by a model we proposed previously in which the channel closing rate, a measure of the stability of the open channel state, controls an apparent tendency of the channel to desensitize, most likely, through the closed channel state. Specifically, the flop sequence of GluR2 promotes the channel to close more rapidly and consequently to desensitize with a faster rate than the flip sequence. For GluR1, the alternative splicing does not seem to affect the channel opening kinetics, since the flip and flop variants of GluR1 have the same channel opening rate, and the same channel closing rate. As expected and indeed observed, the flop variant desensitizes with the same rate as the flip variant does. On the basis of these results, we hypothesize that the flip/flop sequence cassette of AMPA receptors, in a sequence-dependent manner, regulates the rate of the channel closing process, in the microsecond time domain, through which it further regulates the channel desensitization in the millisecond time region.

Each of the four α-amino-3-hydroxy-5-methyl-4-isoxazolepropionic acid (AMPA)[1] glutamate receptors, i.e., GluR1−4 or GluRA−D, is alternatively spliced in the extracellular region, generating the "flip" and "flop" variants (*1*). The alternative splicing correlates to a 38-amino acid sequence encoded by a 115 bp region but results in a difference of only 9−11 amino acids (*1*) or ∼1% of the overall amino acid content (*2*). The flip/flop sequence cassette is part of the extracellular ligand binding domain, and the C-terminus of this sequence cassette precedes the last transmembrane domain or the M4 domain (*3*) (Figure 1). Alternative splicing has been hypothesized to contribute to the functional heterogeneity of AMPA receptor-mediated synaptic transmission (*3*−*5*). In the brain, the flip and flop isoforms are differentially expressed in cell-type- and age-specific manners (*1, 6*−*10*). Furthermore, native AMPA receptors are heteromeric receptor assemblies of different subunits that may have different flip and flop isoforms (*1*). At the receptor level, the flip and flop variants of an AMPA receptor subunit generally have different kinetic properties. The flop variants of GluR2−4 desensitize (i.e., become inactivated when glutamate remains bound to the receptors) at least 3 times faster but recover more slowly from desensitization than the flip counterparts (*6, 11*). However, the flip and flop isoforms of GluR1 desensitize with an identical rate at a given glutamate concentration (*6, 11, 12*). In spite of a wealth of information about the alternative splicing, whether it affects the rate of a receptor channel opening through which a synaptic signal is transmitted is not known.

To address this question, we previously characterized the kinetic mechanism of channel opening for the flip and flop variants of $GluR3_{flip}$ (*13*), using a laser-pulse photolysis approach with a caged glutamate [i.e., γ-*O*-(α-carboxy-2-nitrobenzyl)glutamate] (*14*). We found that the GluR3 flop variant opens its channel, upon binding of glutamate, with the same rate as the flip variant does but closes its channel almost 4-fold faster (*13*). We have therefore hypothesized that the functional role of the flip/flop sequence module in the channel opening kinetic process is to regulate the lifetime of the open channel or the stability of the open channel conformation (*13*). Furthermore, our study of the channel opening kinetic mechanism of a leucine-to-tyrosine substitution mutant or $GluR1_{flip}$ L497Y (*15*) suggested that the channel closing rate appears to be linked to desensitization in that the faster an open channel closes, the faster the channel desensitizes, which is most consistent with a mechanism by which the channel desensitizes through the closed channel state (*16*).

[†] This work was supported in part by grants from the Department of Defense, National Institutes of Health, the ALS Association, and the Muscular Dystrophy Association (to L.N.). Z.H. is supported by a postdoctoral fellowship from the Muscular Dystrophy Association.

* To whom correspondence should be addressed. Telephone: (518) 591-8819. Fax: (518) 442-3462. E-mail: lniu@albany.edu.

[1] Abbreviations: AMPA, α-amino-3-hydroxy-5-methyl-4-isoxazolepropionic acid; caged glutamate, γ-*O*-(α-carboxy-2-nitrobenzyl)glutamate; HEK-293 cells, human embryonic kidney cells.

10.1021/bi8015907 CCC: $40.75
Published on Web 03/10/2009

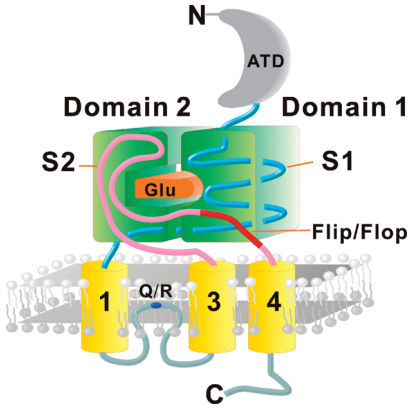

FIGURE 1: Schematic drawing of the topology of an AMPA receptor subunit showing the sequence location of the alternatively spliced flip/flop region. Each subunit consists of an extracellular N-terminal domain (ATD), S1 and S2 ligand binding domains, three transmembrane segments (TM1, -3, and -4), an re-entrant loop (TM2) containing the Q/R RNA editing site (in GluR2), and an intracellular C-terminal domain. The ligand-binding core whose crystal structure has been determined is comprised of S1 and S2 domains. For GluR2, the S1 and S2 domains correspond to residues 392−506 and 632−775, respectively (*37, 38*). The flip/flop sequence forms part of the ligand binding core, according to the crystal structure (*37, 38*). In the flip/flop sequence cassette of 38 amino acids, there are nine amino acid residues that are actually different. The S1S2 domain contains the first five variable residues between the flip and flop variants but lacks the last six residues, four of which belong to the variable residues between the flip and flop isoforms. A segment of 10 amino acid residues links the C-terminal end of the flip/flop sequence cassette to the last putative transmembrane region (TM4).

To further test this hypothesis, we characterized, and report here, the channel opening kinetic constants for the flip and flop variants of the GluR1 and GluR2Q receptors. We chose to characterize the alternatively spliced variants of these two subunits because the flop variant of GluR2Q is known to desensitize more rapidly than its flip counterpart, similar to the GluR3 flip and flop isoforms, whereas the flop variant of GluR1 desensitizes with the same rate as the flip isoform (*6, 11, 12*). On the basis of our hypothesis (*13, 16*) and the difference in the rate of channel desensitization between the two flip/flop pairs of GluR1 and GluR2, we predicted that (a) for GluR2, the flop variant would have the same k_{op} value with the flip isoform but a larger k_{cl} or a faster channel closing rate process and (b) for GluR1, there would be no difference in k_{op} or k_{cl} between the flip and flop variants. What we find, described below, is entirely consistent with our prediction.

EXPERIMENTAL PROCEDURES

Cell Culture and Receptor Expression. To study a specific receptor isoform of GluR1 and GluR2Q, we transiently expressed the homomeric receptor channel in the human embryonic kidney (HEK-293S) cells (*13*) as a heterologous expression system. For the transfection of a receptor gene in HEK-293 cells, the cDNAs encoding the flip and flop variants of the rat GluR1 and GluR2Q receptors separately in the pBluescript vector, which we obtained from S. Heinemann's laboratory, were individually cloned into the pcDNA3.1 vector (Invitrogen, Carlsbad, CA). The HEK-293S cells were cultured in Dulbecco's modified Eagle's medium supplemented with 10% fetal bovine serum in a 37 °C, 5% CO_2, humidified incubator. The transient transfection followed a calcium phosphate protocol, described previously (*13*), and the cells were used for electrophysiological recording 48 h after transfection.

$$A + nL \underset{}{\overset{K_1}{\rightleftharpoons}} AL_n \underset{k_{cl}}{\overset{k_{op}}{\rightleftharpoons}} \overline{AL_n}$$

FIGURE 2: A general mechanism of channel opening for AMPA receptors. In the scheme, A represents the active, unliganded form of the receptor, L the ligand or glutamate, AL_n the closed channel states with n ligand molecules bound, and $\overline{AL_n}$ the open channel state. The number of glutamate molecules that bind to the receptor and to open its channel, n, can be from one to four, assuming that a receptor is a tetrameric complex, and each subunit contains one glutamate binding site. It is further assumed that a ligand does not dissociate from the open channel state. k_{op} and k_{cl} are the channel opening and channel closing rate constants, respectively. For simplicity and without contrary evidence, it is assumed that glutamate binds with equal affinity or K_1, the intrinsic equilibrium dissociation constant, at all binding steps. Further discussion of the mechanism is presented in the text.

Whole-Cell Recording and Laser-Pulse Photolysis. The whole-cell current response to glutamate was recorded at −60 mV and 22 °C, as described previously (*17*). Briefly, the electrode resistance was ~3 MΩ when filled with the electrode solution: 110 mM CsF, 30 mM CsCl, 4 mM NaCl, 0.5 mM $CaCl_2$, 5 mM EGTA, and 10 mM HEPES (pH 7.4 adjusted by CsOH). The external bath solution contained 150 mM NaCl, 3 mM KCl, 1 mM $CaCl_2$, 1 mM $MgCl_2$, and 10 mM HEPES (pH 7.4). Current traces were sampled at a 5−50 kHz frequency and filtered at 2−20 kHz by an eight-pole Bessel filter, using an Axopatch 200B (MDS Analytical Technologies). pCLAMP 8 (MDS Analytical Technologies) was used for acquisition of data. In the laser-pulse photolysis measurements, the caged glutamate (Invitrogen) was photolyzed using a 355 nm laser pulse delivered by a Minilite II pulsed Q-switched Nd:YAG laser (Continuum). A concentration of photolytically released glutamate that activated the receptor response was estimated by using two free glutamate solutions with known concentrations to calibrate the current amplitudes from the same cell before and after a laser photolysis, as described previously (*13, 16*). Both free glutamate and the caged glutamate solution were delivered by using a U-tube flow device (*13, 16*).

Data Analysis. The observed rate constant, k_{obs}, for the opening of the channel according to a general mechanism (Figure 2) was formulated as in eq 1.

$$k_{obs} = k_{cl} + k_{op}\left(\frac{L}{L + K_1}\right)^n \quad (1)$$

All other terms in eq 1 are defined either in the text or in the legend of Figure 2. In the derivation of eq 1, the rate of ligand binding was assumed to be fast relative to the rate of channel opening. This assumption was supported by the fact that the whole-cell current rise observed in the laser-pulse photolysis measurement was adequately described by a single first-order rate law, as in eq 2 below, over the entire range of glutamate concentrations not only in this study (see the results in the text) but also in all of our previous studies of AMPA receptor channel opening mechanisms (*13, 16*−*19*).

$$I_t = I_A(1 - e^{-k_{obs}t}) \quad (2)$$

By eq 2, the k_{obs} at a given glutamate concentration was calculated. In eq 2, I_t and I_A represent the whole-cell current amplitude at time t and the maximum current amplitude, respectively. Furthermore, a set of k_{cl} and k_{op} values as well as K_1 corresponding to a particular number of ligand(s) bound, i.e., $n = 1-4$ (see the legend of Figure 2), was obtained from k_{obs} as a function of glutamate according to eq 1. In addition, K_1 was estimated independently from the dose−response relationship, in eq 3, derived also from the general mechanism of channel opening (because there is an equation below).

$$I_A = I_M R_M \frac{L^n}{L^n + \Phi(L + K_1)^n} \quad (3)$$

where I_M is the current per mole of receptor, R_M the number of moles of receptor on the cell surface, and Φ^{-1} the channel opening equilibrium constant.

In addition, a Φ value defined by eq 4 below was estimated from a set of k_{cl} and k_{op} values, which was obtained from eq 1 for each of the alternatively spliced variants by Φ-value analysis (*20*−*22*). The use of the Φ-value analysis allowed us to estimate the change in the free energy for the transition state for each receptor channel differing by the alternatively spliced sequence (*16*), in eq 4 (because there is an equation below).

$$\Phi = \frac{\Delta\Delta G_{TS-C}}{\Delta\Delta G_{O-C}} \quad (4)$$

where the $\Delta\Delta G$ value was calculated on the basis of eq 5, using k_{op} and k_{cl} values associated with the flip and flop variants.

$$\Delta G^{\ddagger} = RT \ln\left(\frac{\kappa T}{hk}\right) \quad (5)$$

In eq 5, R is the gas constant, T the temperature in kelvin, h Planck's constant, κ the Boltzmann constant, and k the rate constant. It should be mentioned, however, that the energy level of the flip isoform was arbitrarily used as the baseline.

For data analysis, linear regression and nonlinear fitting were performed using Origin 7 (OriginLab, Northampton, MA). Furthermore, Simplex and Levenberg−Marquardt algorithms were used in nonlinear fitting. Unless otherwise noted, at least triplicate data from three cells were collected and used for data analysis.

RESULTS

Dependence of Desensitization Rate Constants on Glutamate Concentration. We first measured the rate constant of channel desensitization as a function of glutamate concentration for the flip and flop variants of GluR1 and GluR2Q, respectively. Here a receptor was expressed transiently in HEK-293 cells, and the glutamate-induced whole-cell current was recorded at −60 mV and pH 7.4. As shown in Figure 3A, a representative whole-cell current response to glutamate rose rapidly due to channel activation and then returned to the baseline due to channel desensitization. The desensitization rate process or the falling phase of the whole-cell current (Figure 3A) could be characterized by a single first-order

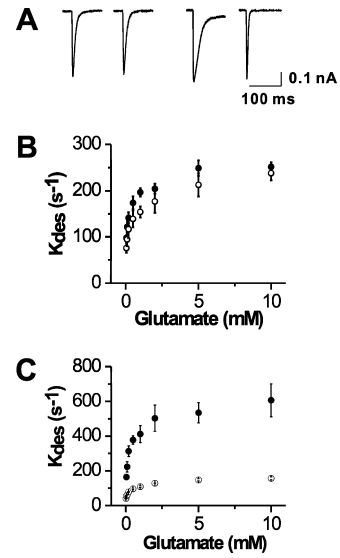

FIGURE 3: Dependence of the desensitization rate constant (k_{des}) on glutamate concentration for the flip and flop channels of both GluR1 and GluR2Q. Each receptor isoform was expressed in HEK-293 cells, and the whole-cell current response to glutamate was recorded at −60 mV, pH 7.4, and 22 °C. (A) Representative whole-cell current responses via GluR1 flip and flop channels (left pair) and GluR2Q flip and flop channels (right pair) to application of 500 μM glutamate. The desensitization rate constants for $GluR1_{flip}$ and $GluR1_{flop}$ are 175 s^{-1} (left trace of the left pair) and 180 s^{-1} (right trace of the left pair) at this glutamate concentration, respectively. The desensitization rate constants for $GluR2Q_{flip}$ and $GluR2Q_{flop}$ are 120 s^{-1} (left trace of the right pair) and 420 s^{-1} (right trace of the right pair) at this glutamate concentration, respectively. (B) Dependence of k_{des} on glutamate concentration for $GluR1_{flop}$ (●) and $GluR1_{flip}$ (○) channels. Each data point is an average of at least three measurements from at least three cells. The standard error of the mean is represented by an error bar. (C) Dependence of k_{des} on glutamate concentration for $GluR2Q_{flop}$ (●) and $GluR2Q_{flip}$ (○) channels.

rate process for >98% of the reaction and over the entire range of glutamate concentrations for all of the receptor isoforms (Figure 3B,C). On the basis of these results (Figure 3B,C), two conclusions can be drawn. First, the desensitization rate constant for both $GluR1_{flop}$ and $GluR2Q_{flop}$, like their respective flip counterparts, was dependent on glutamate concentration in that the receptor channels desensitized with a faster rate with an increase in glutamate concentration. Moreover, at a sufficiently high concentration of glutamate (e.g., 10 mM), the desensitization rate constant reached a plateau (Figure 3B,C). Second, comparison of the desensitization rate constant between a flip/flop pair showed that for GluR1, the flip and flop channels desensitized with an identical rate at any given glutamate concentration (Figure 3B), whereas for GluR2Q, the flop isoform desensitized ~3-fold faster than the flip isoform (Figure 3C). These observations are consistent with those previously reported for these receptors (*1, 6, 11, 12, 15, 23*).

Dose−Response Relationship. We then asked if the K_1 value (i.e., the intrinsic equilibrium dissociation constant of the ligand in the mechanism of channel opening (in Figure 2)), and the EC_{50} value (i.e., the ligand concentration that corresponds to 50% of the maximum response) of these flop isoforms would be different from the respective values of their flip counterparts. By using eq 3, the K_1 values for $GluR1_{flop}$ and $GluR2Q_{flop}$ were determined to be 0.45 ± 0.04 and 1.14 ± 0.14 mM, respectively, with $n = 2$ from the

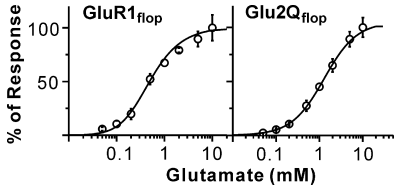

FIGURE 4: Dose−response relationship of $GluR1_{flop}$ (left) and $GluR2Q_{flop}$ (right) to glutamate. The whole-cell current response of a receptor to various glutamate concentrations was measured from HEK-293 cells. Each data point is an average of at least three measurements from at least three cells. The standard error of the mean is represented by an error bar. The current response from a single cell to 1 mM glutamate was used as the control, and the current amplitude at 10 mM was set to be 100%. The observed whole-cell current was corrected for desensitization (*13*,*16*). The best-fit parameters using eq 3 (solid line) that corresponded to $n = 2$ yielded a K_1 of 0.45 ± 0.04 mM for $GluR1_{flop}$ and a K_1 of 1.14 ± 0.14 mM for $GluR2Q_{flop}$. A complete list of fits using different n values is given in Table 1.

respective dose−response curves (see Figure 4, and also see Table 1 for the fits using different n values). As an independent evaluation of the dose−response data, we further determined the EC_{50} value using the Hill equation (*24*): $EC_{50} = 0.53 \pm 0.06$ mM and the Hill coefficient = 1.2 for $GluR1_{flop}$, and $EC_{50} = 1.46 \pm 0.05$ mM and the Hill coefficient = 1.1 for $GluR2Q_{flop}$. These results suggest that EC_{50} is similar to K_1 numerically at $n = 2$ (note that the Hill equation does not restrict the number of the ligand molecules bound). Furthermore, both EC_{50} and K_1 values for each of the flop isoforms were in agreement with the corresponding values of the flip isoforms for GluR1 (*23, 25, 26*) and GluR2 (*11*) reported previously, including the values we determined (*17, 18*). It should be noted that our study of GluR3 flip and flop isoforms showed a similar EC_{50} and a similar K_1 (*13*). Koike et al. (*11*) also reported that the flip and flop isoforms of GluR2Q have the same EC_{50} value in a study which used a fast solution exchange technique with outside-out patches isolated from a *Xenopus* oocyte membrane. On the basis of the magnitude of K_1 values of all of the flip and flop variants of the three receptor subunits, the alternative splicing responsible for generating the flip and flop isoforms in the AMPA receptors does not appear to affect the ligand binding affinity.

Channel Opening Rate Constants. Next we measured the channel opening (k_{op}) and channel closing rate constants (k_{cl}). To do this, we used a laser-pulse photolysis technique with the caged glutamate, which liberated free glutamate upon photolysis with a $t_{1/2}$ of ~30 μs (*14*). Laser-pulse photolysis of the caged glutamate triggered a rapid increase in whole-cell current (Figure 5A). As shown (solid line, in Figure 5A), the rising phase could be adequately described by a single-exponential rate process, which reflected a rapid channel opening (see the explanation of the channel opening mechanism below). Accordingly, the observed rate constant of channel opening, k_{obs}, at a concentration of photolytically generated glutamate was calculated using eq 2. From the plot of k_{obs} versus the concentration of glutamate, we determined the k_{op} and k_{cl} values for both $GluR1_{flop}$ (Figure 5B and Table 2) and $GluR2Q_{flop}$ (Figure 5C and Table 2), using eq 1. Specifically, the best fit of k_{obs} as a function of glutamate concentration using eq 1, assuming $n = 2$, yielded k_{op} and k_{cl} values of $(2.7 \pm 0.2) \times 10^4$ and $(2.2 \pm 0.2) \times 10^3$ s^{-1} for $GluR1_{flop}$ and $(8.6 \pm 0.4) \times 10^4$ and $(3.7 \pm 0.1) \times 10^3$ s^{-1} for $GluR2Q_{flop}$, respectively, in addition to their corresponding values of k_{op} and k_{cl} for the flip variants, which we have determined previously (*17, 18*). The rate constants for the flip and flop variants of GluR1 and GluR2, together with the corresponding values of GluR3, which we reported previously (*13*), are summarized in Table 3. By comparison of k_{op} and k_{cl} for a flip/flop pair (as in Figure 5B,C and Table 3), it is apparent that the alternative splicing did not affect the channel opening rate process for any receptor subunits mentioned above. However, like GluR3 (*13*), the GluR2Q flop variant closed the channel faster than the flip isoform, whereas $GluR1_{flop}$ closed the open channel with the same rate as the $GluR1_{flip}$ isoform.

Several features in our measurements of the channel opening kinetic process are worth noting. First, the rising phase of the current (in Figure 5A) obeyed a single-exponential rate process over the entire concentration range of glutamate (i.e., 80−260 μM). This observation was consistent with the assumption that the channel opening rate or the rate of transition from the closed channel form (i.e., AL_n) to the open channel form (i.e., $\overline{AL_n}$) was slow compared with the rates of all preceding steps involving glutamate binding (see Figure 2) but was inconsistent with the assumption that the channel opening rate was either comparable to or faster than the ligand binding rate. In the latter scenarios, a single-exponential rate process would be inadequate for describing the rising phase kinetics over the range of concentrations we have used (*17, 18*). Therefore, by the assumption that the channel opening rate was the rate-limiting step, eq 1 was derived from the kinetic mechanism of channel opening (in Figure 2). Furthermore, the plot of k_{obs} as a function of glutamate concentration by eq 1 was supposed to be linear over the range of glutamate concentrations we have determined (Figure 5B,C). We note, however, that it was not possible, in this study, to measure the rate of channel opening or k_{obs} over the full range of glutamate concentrations or up to saturation to calculate k_{op} and k_{cl} using eq 1. Our measurement was limited largely by a relatively fixed concentration of glutamate liberated from laser-pulse photolysis without destroying the cell or the tight seal of recording, yet that concentration was not sufficiently high as compared to the EC_{50} values of the receptor channels we studied (i.e., most of them were in the millimolar range). However, using a mutant receptor (i.e., GluR1 L497Y and its EC_{50} value of ~50 μM), we were able to determine k_{obs} even at saturating glutamate concentrations, where the linear relationship of k_{obs} as a function of glutamate concentration (as in the form of eq 1) continued to hold (*16*). Furthermore, we found that the k_{op} and k_{cl} values obtained from a limited range of data points (i.e., the lower 20%, which was comparable to the range we could measure in this study) were identical, within the experimental error, with those obtained using the entire data set.

It should be noted, however, that eq 1 cannot be used to calculate k_{op} and k_{cl} from k_{obs} when the glutamate concentration becomes sufficiently low that glutamate binding becomes rate-limiting (*17*), since ligand binding is a bimolecular process. To ensure that the ligand binding was always fast so that the relatively slow channel opening rate process was observed and measured, the lowest fraction of the open channel form at which we measured the k_{obs} to be included in calculating channel opening rate constants was chosen to

Table 1: K_1 Values Estimated from the Dose−Response Curve for $GluR1_{flop}$ and $GluR2Q_{flop}$

	$GluR1_{flop}$				$GluR2Q_{flop}$			
n	K_1 (mM)	Φ	I_MR_M (nA)	R^2	K_1 (mM)	Φ	I_MR_M (nA)	R^2
1	1.83 ± 0.35	0.51 ± 0.10	158.0 ± 15.4	0.989	6.19 ± 0.52	160.0 ± 4.8	0.36 ± 0.02	0.999
2	0.45 ± 0.04	0.61 ± 0.12	158.1 ± 4.0	0.992	1.14 ± 0.14	160.9 ± 16.4	0.52 ± 0.11	0.992
3	0.24 ± 0.03	0.71 ± 0.20	166.6 ± 23.3	0.988	0.60 ± 0.09	175.8 ± 30.0	0.68 ± 0.22	0.985
4	0.16 ± 0.02	0.77 ± 0.25	171.0 ± 28.9	0.985	0.41 ± 0.07	180.7 ± 37.4	0.74 ± 0.28	0.980

Table 2: k_{op} and k_{cl} Values for $GluR1_{flop}$ and $GluR2Q_{flop}$ (n = 1−4)

	$GluR1_{flop}$			$GluR2Q_{flop}$		
n	k_{op} ($\times 10^4$ s^{-1})	k_{cl} ($\times 10^3$ s^{-1})	R^2	k_{op} ($\times 10^4$ s^{-1})	k_{cl} ($\times 10^3$ s^{-1})	R^2
1	3.72 ± 0.30	1.13 ± 0.23	0.961	9.54 ± 0.60	2.82 ± 0.16	0.972
2	2.73 ± 0.23	2.19 ± 0.16	0.956	8.56 ± 0.44	3.73 ± 0.09	0.981
3	2.46 ± 0.22	2.50 ± 0.14	0.952	9.54 ± 0.50	3.99 ± 0.09	0.980
4	2.35 ± 0.22	2.65 ± 0.13	0.949	10.63 ± 0.62	4.12 ± 0.09	0.976

be ~4% (for $GluR1_{flip}$ and $GluR2Q_{flip}$, the 4% fraction of the open channel form corresponded to 40 and 100 μM glutamate, respectively; the difference here is due to their different K_1 values or approximately their EC_{50} values) (*17, 18*). Three lines of evidence supported the assumption that the 4% fraction of the open channel form was sufficiently high such that the rate constant we measured pertained to the channel opening rate rather than ligand binding rate process. Three lines of evidence support the lower limit of k_{obs} to be used with eq 1. First, the estimate of k_{cl} from eq 1, including from the use of the k_{obs} value at low glutamate concentrations ($k_{obs} \approx k_{cl}$ when $L \ll K_1$, as shown from the reduction of eq 1), yielded values similar to the lifetimes determined by single-channel recording ($k_{cl} = 1/\tau$, where τ is the lifetime expressed as a time constant) for both $GluR1_{flip}$ (*17, 25*) and $GluR2Q_{flip}$ (*18, 27*). Second, at glutamate concentrations much lower than 100 μM for $GluR2Q_{flip}$, the k_{obs} values we measured deviated significantly from the linear relationship predicted by eq 1 (unpublished data of G. Li and L. Niu). Third, the rate of the rise time which reflected ligand binding was also observed qualitatively in the GluR6Q kainate receptor when the glutamate concentration was very low, where a rapid solution exchange technique was even possible to measure the rate of the slow current rise (*28*). In our case, however, the k_{obs} values measured from glutamate concentrations equal to or greater than 4% of the fraction of the open channel form held a linear relationship, as shown in eq 1, for all of the AMPA receptor channels we have measured, including the $GluR1_{flip}$ L497Y mutant, where the linear relationship was tested using k_{obs} values from a full range of glutamate concentrations (*16*).

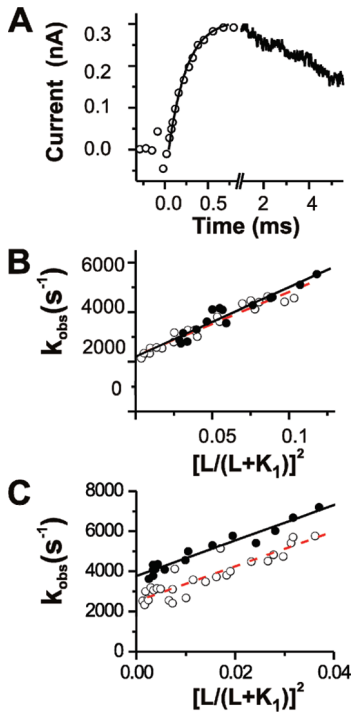

FIGURE 5: Laser-pulse photolysis measurement of the channel opening kinetics for the flip and flop channels of GluR1 and GluR2Q. (A) A representative whole-cell current from the opening of the $GluR1_{flop}$ channel initiated by a laser-pulse photolysis of caged glutamate at time zero, with a HEK-293 cell voltage clamped at −60 mV, pH 7.4, and 22 °C. For clarity of illustration, the number of the data points was reduced in the rising phase of the current. The whole-cell current rise was fitted by a single-exponential rate equation (i.e., eq 2), shown as the solid line, yielding a k_{obs} of 5400 s^{-1} at 200 μM photolytically liberated glutamate. Note that the direction of the current response was plotted opposite to that recorded. (B) Plot of k_{obs} vs glutamate concentration for the channel opening rate reaction of GluR1 flip (○) and flop (●) channels. Each data point represents one k_{obs} value obtained at a particular concentration of photolytically released glutamate. Using eq 1, the k_{cl} and k_{op} value were determined to be (2.2 ± 0.2) × 10^3 and (2.7 ± 0.2) × 10^4 s^{-1} for $GluR1_{flop}$ and (2.2 ± 0.1) × 10^3 and (2.6 ± 0.1) × 10^4 s^{-1} for $GluR1_{flip}$, respectively, with n = 2. (C) Likewise, the best fit of k_{obs} vs glutamate concentration at n = 2 yielded k_{cl} and k_{op} values of (3.7 ± 0.1) × 10^3 and (8.6 ± 0.4) × 10^4 s^{-1} for $GluR2Q_{flop}$ (●) and (2.6 ± 0.1) × 10^3 and (8.7 ± 0.8) × 10^4 s^{-1} for $GluR2Q_{flip}$ (○), respectively. A complete list of fits using different n values is given in Table 2.

Table 3: Summary of k_{op} and k_{cl} Values at n = 2 for the Flip and Flop Variants of GluR1, -2, and -3 AMPA Receptors

AMPA	k_{op} ($\times 10^4$ s^{-1})	k_{cl} ($\times 10^3$ s^{-1})	K_1 (mM)	R^2
$GluR1_{flop}$	2.7 ± 0.2	2.2 ± 0.2	0.5 ± 0.1	0.96
$GluR1_{flip}$	2.6 ± 0.1	2.2 ± 0.1	0.5 ± 0.1	0.97
$GluR2Q_{flop}$	8.6 ± 0.4	3.7 ± 0.1	1.1 ± 0.1	0.98
$GluR2Q_{flip}$	8.7 ± 0.8	2.6 ± 0.1	1.3 ± 0.1	0.91
$GluR3_{flop}$	9.9 ± 0.5	3.8 ± 0.1	1.0 ± 0.7	0.97
$GluR3_{flip}$	9.6 ± 1.1	1.1 ± 0.2	1.0 ± 0.7	0.91

DISCUSSION

This study shows that the alternatively spliced, flip/flop sequence cassette differentially affects the channel opening kinetic process of AMPA receptors. The flop sequence of GluR2 correlates to a channel that closes faster than its flip counterpart, without affecting the rate of opening of the

channel in response to binding of glutamate, whereas for GluR1, the flip/flop sequence cassette does not affect either the channel opening or the channel closing rate process. A detailed comparison of these results (in Table 3) with those of the flip variant of GluR1 (*17*) and GluR2 (*18*) as well as the flip/flop pair of GluR3 we reported earlier (*13*) implicates possible roles of alternative splicing in both channel gating and the structure−function relationship of the AMPA receptors. However, before we discuss the possible functional implication of alternative splicing on channel opening, we first discuss the channel opening mechanism based on which the channel opening and channel closing rate constants were obtained.

Channel Opening Mechanism. The characterization of k_{op} and k_{cl} using eq 1, which was derived from the mechanism of channel opening (Figure 2), was based on the rapid kinetic measurement of the channel opening rate constant or k_{obs} using eq 2, without the complication of channel desensitization. This is different from other kinetic mechanisms that describe the channel opening, such as the one used for kinetic analysis of the flip and flop variants of GluR2Q (*11*), in that channel desensitization is linked to the channel opening mechanism. As such, the estimate of the rate constants of channel opening will have to rely on the measurement of the channel desensitization and deactivation. In our experiment, however, the channel opening reaction was measured virtually cleanly from the rising phase of the current response, because the desensitization reaction could not have proceeded appreciably during the current rise even if binding of glutamate had driven the channel to desensitize, concurrent with channel opening (*29, 30*). For example, a k_{obs} of 5400 s^{-1}, calculated from the current rise for the $GluR1_{flop}$ channel opening (Figure 5A), was ~40 times larger than the apparent rate of desensitization of 140 s^{-1} (Figure 3B) at the same glutamate concentration, i.e., 200 μM. As such, when the current increased to 95%, during which the k_{obs} of 5400 s^{-1} was calculated, the desensitization reaction with a rate constant of 140 s^{-1} proceeded only ~6%. Thus, the kinetic process that occurred within the current rise in the laser-pulse photolysis measurement was dominated by the channel opening reaction, and its rate constant could be calculated by a simple, distinct kinetic rate expression (i.e., eq 2) separate from the desensitization reaction. This was also confirmed by the fact that a simultaneous fit of both the rising and falling phases (Figure 5A) by two first-order rate equations, one representing channel opening and the other representing desensitization, returned a k_{obs} value that was no different (i.e., ±5% error range) from the one obtained by using only a single-exponential fit of the rising phase (using eq 2).

By the mechanism of channel opening (Figure 2), our data analysis using eq 1, yielding k_{op} and k_{cl} values, was carried out with all possible n values ($n = 1-4$), where the maximal n value of 4 was based on the assumption that an AMPA channel is a tetramer (*31*), and each subunit contains one glutamate binding site. As seen in Figure 5B,C and Table 2, the fitting of k_{obs} versus glutamate concentration by eq 1, like the fitting of the dose−response relationship by eq 3 as in Figure 4 and Table 1, was statistically identical when $n = 1-4$. Although the fitting result based on the data of this study did not allow us to rule out the possibility that binding of one glutamate molecule per receptor complex (i.e., $n = 1$) would be sufficient to open the channel, we prefer that the k_{op} and k_{cl} values we obtained from fitting be assigned to $n = 2$ as the minimal number of ligand molecules to open the receptor channel. Choosing $n = 2$ as the minimal number of ligand molecules per receptor complex was consistent with additional lines of evidence from our study using a mutant receptor, i.e., $GluR1_{flip}$ L497Y, in which the fitting of k_{obs} over the entire glutamate concentration range showed that $n = 1$ was not satisfactory, whereas the k_{op} value remained invariant when $n = 2-4$ (*16*). The study of this mutant was designed to address, among other questions, the minimal number of glutamate molecules that must bind and open the channel. Furthermore, the results by others suggested that binding of two glutamate molecules per receptor complex is sufficient to open an AMPA receptor channel (*31, 32*), although binding of one glutamate molecule is sufficient to only desensitize the channel (*33*).

We should emphasize that the k_{cl} value for both $GluR1_{flop}$ and $GluR2Q_{flop}$, obtained from the fitting (Figure 5B,C and Table 2), and the subsequent conclusion based on the comparison of these values with those from the corresponding flip variants (see discussion below), could be estimated independently or without any knowledge of the n value(s). This is because when $L \ll K_1$ or at low agonist concentrations, eq 1 was reduced to $k_{cl} \approx k_{obs}$, suggesting that an observed rate constant measured at a low glutamate concentration was approximately reflective of the k_{cl} for the same channel. Specifically, at the lower end of the glutamate concentration range (but not at the lowest glutamate concentration to prevent the measurement of ligand binding rate, as described earlier), a k_{obs} of ~2100 s^{-1} for $GluR1_{flop}$ (Figure 5B) and of ~3700 s^{-1} for $GluR2Q_{flop}$ (Figure 5C) provided a rough estimate of k_{cl} for each channel. As expected, the estimate of k_{cl} using k_{obs} at low glutamate concentrations was in good agreement with our analysis of k_{cl} at $n = 2$ by using eq 1 and from a set of k_{obs} values as a function of glutamate concentration (see Table 2).

Alternative Splicing Regulates the GluR2 Channel Opening Process by Affecting k_{cl}. It is useful to characterize k_{op} and k_{cl} for a channel (*13*), because the magnitudes of k_{op} and k_{cl} establish quantitatively how fast the channel opens, following the binding of agonist, and how quickly the open channel closes, which is a measure of the lifetime of the open channel or τ, since $k_{cl} = 1/\tau$ (*17*). For GluR2, the k_{op} for the flop variant is identical, within experimental error, to that of the flip counterpart (see Table 3). In contrast, the k_{cl} of $(3.7 \pm 0.1) \times 10^3$ s^{-1} for the flop variant is ~1.5-fold larger than the value of $(2.6 \pm 0.1) \times 10^3$ s^{-1} for the flip isoform (*18*), suggesting that the open channel of the flop isoform closes ~1.5-fold faster. Therefore, the alternative splicing in GluR2, reflected by a difference of nine amino acids in the flip/flop sequence cassette, affects the channel opening kinetic properties of these variants by regulating how quickly the open channel closes.

The relationship between the rate constants and the energetics of the transition from the closed to open channel state can be rationalized in a broader context using the Φ-value analysis method (*20−22*). We have previously applied this method to the analysis of the channel opening rate constants of the alternatively spliced variants of the GluR3 subunit (*13*) and a leucine-to-tyrosine substitution mutant of GluR1 (i.e., $GluR1_{flip}$ L497Y) (*16*). By the

Φ-value analysis, which is used to infer transition state structures from changes in kinetics due to a sequence variation (*20*−*22*), we proposed that the change in the free energy of the open channel state affects its stability and alters the channel closing rate constant, and vice versa (*13*). Specifically, for GluR2, the Φ-value analysis (eqs 4 and 5) of the free energy for the transition from the closed channel to the open channel state for both flip and flop gives rise to a value of zero (see Figure 6 and its legend), indicating that the structure formed by the flop sequence is as much native at the flip/flop sequence site, i.e., the 38-amino acid segment, as it is formed by the flip sequence. In other words, the flip/flop sequence cassette does not affect the transition from the closed channel to the open channel state. Therefore, if the open channel state of the flip variant is used as the reference, the flop variant is 0.22 ± 0.06 kcal/mol less stable (see the legend of Figure 6). Thus, the flop channel spends less time dwelling on the open channel state, relative to the flip channel, so that it closes more quickly (Figure 6). It should be noted that the activation energy for the closed-open transition has not been previously determined. Using the same free energy diagram, the flip and flop variants of GluR3 exhibit a similar energetic profile whereas the GluR1 L497Y mutant shows exactly the opposite, as we reported previously (*13, 16*) (see the legend of Figure 5; for the flip/flop pair of GluR1, see the legend and the discussion below). Previously, a similar method (i.e., Brønsted plot) has been used to understand the channel gating kinetics and/or equilibrium linear free energy relationships for the nicotinic acetylcholine receptor (*34*).

Because the flip/flop sequence cassette in GluR2, like the GluR3 flip/flop pair, affects the channel closing rate constant or the lifetime of the open channel, we hypothesize that the flip/flop sequence cassette has a significant structural role in stabilizing the open channel conformation (*13*). The presumptive structural role of the flip/flop sequence cassette may be linked to its unique location, in the overall receptor topology, as the flip/flop sequence precedes the putative fourth transmembrane (*3*). Therefore, it is possible that the flip/flop sequence cassette provides an important structural link from the extracellular ligand binding domain to the membrane-embedded M4 domain and is therefore involved in stabilizing the extracellular domain, when bound with glutamate, so that the sequence cassette is able to influence the stability of the open channel conformation (*35, 36*).

In the crystal structure of the S1S2 extracellular binding domain, the flip/flop sequence cassette is seen to extend into the ligand binding core and to form part of the D1 (upper lobe)−D1 dimer interface (*37, 38*). The D1−D1 dimer interface is therefore thought to be important in stabilizing the open channel conformation (*37*−*39*). Following glutamate binding, domain closure occurs. Originating from the same ligand-bound, domain-closed structure are two parallel pathways (*37*). In the first pathway, the D1−D1 dimer interface, formed between two protomers, remains intact, and the conformational strain caused by domain closure between D1 and D2, formed within the same protomer (i.e., the closed channel state has an open cleft between D1 and D2, but with the constrained dimer interface), is translated to the gate within the lipid bilayer, thus opening the channel (i.e., the open channel state has a closed cleft between D1 and D2, and constrained dimer interface). It should be noted that in this pathway, the closed and open states share the same D1−D1 dimer interface. In the second pathway or the one leading to channel desensitization, the domain-closed structure (i.e., closed channel state with an open cleft, but with a constrained dimer interface) undergoes domain interface rupture, sending the receptor into the desensitized state (i.e., closed cleft between D1 and D2, but with the relaxed dimer interface) (*37*). Therefore, on the basis that part of the flip/flop sequence forms the dimer interface and that the interface affects the stability of the open channel conformation (*37, 38*), a change in k_{cl} is consistent with a change in the stability of the interface. Furthermore, if the flip sequence of GluR2 is used as the benchmark, our interpretation of the difference in k_{cl} between the GluR2 flip and flop isoforms in the context of the channel activation/desensitization model, as described by Sun et al. (*37*), is that the flop sequence corresponds to a weakened structural support in stabilizing the D1−D1 domain interface in the open channel state such that the reopening of the D1−D2 closed cleft in the open state to return to the open cleft between D1 and D2 in the closed channel state is kinetically more favorable.

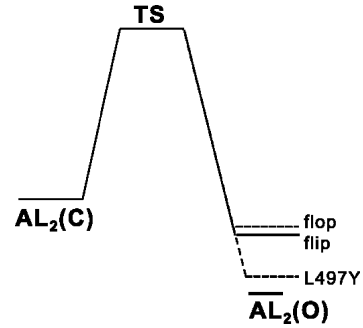

FIGURE 6: Free energy diagram for the transition from the closed channel state (C) to the open channel state (O) of AMPA receptors. The individual free energy change at 22 °C is calculated using eq 5 (Experimental Procedures). The change in the free energy for the transition from the closed to the open state was calculated from a k_{op} value, whereas the change in the free energy for the transition from the open to the closed state was calculated from a k_{cl} value. Specifically, $\Delta G^{\ddagger}_{k_{op}}$ is calculated to be 10.61 ± 0.05 and 10.62 ± 0.03 kcal/mol for GluR2Q$_{flip}$ and GluR2Q$_{flop}$, respectively, whereas the $\Delta G^{\ddagger}_{k_{op}}$ values for GluR2Q$_{flip}$ and GluR2Q$_{flop}$ are 12.67 ± 0.02 and 12.46 ± 0.01 kcal/mol, respectively. The free energy diagram is then constructed as shown, on the basis of the difference between the values of $\Delta G^{\ddagger}_{k_{op}}$ and $\Delta G^{\ddagger}_{k_{cl}}$ for GluR2Q$_{flip}$. The free energy diagram of GluR2Q$_{flop}$ is likewise constructed and superimposed onto the flip one (the only difference is seen in the difference of the free energy change of the open channel state). Using the free energy change of GluR2Q$_{flip}$ as the reference, $\Delta\Delta G_{TS-C}$ or $\Delta G^{\ddagger}_{k_{op}}$(flop) − $\Delta G^{\ddagger}_{k_{op}}$(flip)] is nearly equal to zero (or 0.01 kcal/mol) for the flop variant; however, $\Delta\Delta G_{O-C}$ or $(\Delta G^{\ddagger}_{k_{cl}} - \Delta G^{\ddagger}_{k_{op}})_{flop} - (\Delta G^{\ddagger}_{k_{cl}} - \Delta G^{\ddagger}_{k_{op}})_{flip}$ of 0.22 kcal/mol is obtained. Consequently, the Φ value yields a value of near zero, using eq 4, for the GluR2Q flip and flop variants. Using the same concept, $\Delta\Delta G_{O-C}$ or $(\Delta G^{\ddagger}_{k_{cl}} - \Delta G^{\ddagger}_{k_{op}})_{flop} - (\Delta G^{\ddagger}_{k_{cl}} - \Delta G^{\ddagger}_{k_{op}})_{flip}$ for the GluR3 flip and flop pair is calculated to be 0.76 kcal/mol (see the rate constants for GluR3 in Table 1); like GluR2, the Φ value is also near zero. It should be noted that the free energy diagram for GluR3, although not drawn here, is qualitatively the same as this diagram for GluR2. In addition, the free energy change for the GluR1 L497Y mutant is shown here, but only schematically, to indicate the stabilizing effect of the mutation on the open channel state, as previously described (*13, 16*). In contrast, the free energy change of the GluR1 flip and flop variants is found to be identical for both the transition state and the open channel state.

Channel Closing and Desensitization. Our previous study of the flip/flop pair of GluR3 and the $GluR1_{flip}$ L497Y mutant channel led us to further hypothesize that the channel closing rate process kinetically regulates the desensitization reaction in that the faster the open channel closes, the faster the channel desensitizes (*16*). By this hypothesis, desensitization begins in parallel to the channel opening reaction but proceeds, with a slower rate, from the closed channel state, once glutamate is bound (*16*). Experimentally, without exception, the rate of channel closing in all of the AMPA receptors we have characterized is markedly faster than the rate of channel desensitization (*13, 17*−*19*). The hypothesis we have proposed represents a simple model that can adequately describe channel desensitization through the closed channel state, which is kinetically controlled by the lifetime of the open channel state, and the model does not require that the channel enter the desensitization reaction from the open channel state. For instance, the flop isoform of GluR2 closes its channel to return to its closed channel state more quickly than the flip isoform; consequently, the flop channel desensitizes more quickly than the flip isoform. The fact that desensitization can still occur, even when a glutamate concentration is too low to open the channel (*33, 40, 41*), supports the notion that the channel can desensitize through the closed channel state. In addition, our hypothesis is consistent with the observations that desensitization is agonist-promoted (*42*), and the L497Y mutant channels can desensitize, albeit very slowly and only at very high concentrations of ligand, as observed by us (*16*) and others (*37, 43*). However, we should emphasize that despite the fact that a simple model can account for our data, i.e., channel closing rate and channel desensitization rate processes are kinetically linked and the channel desensitizes via the closed state, our data do not rule out models of desensitization that may require different or additional steps, including one by which the channel can desensitize through both the open and the closed states (*38*), and models of desensitization that may involve different factors, such as stability of binding cleft (*44*) and state-dependent electrostatic interactions (*45*). Clearly, additional studies in the field are needed for a better understanding of channel desensitization.

The functional role of the flip/flop cassette of GluR2 in desensitization via the closed channel state as we proposed can be also explained in the context of a structural model proposed by Sun et al. (*37*). As compared to the flip sequence, the flop isoform can open the channel with the same rate. However, the open channel state (i.e., the state with the closed cleft between D1 and D2, and constrained dimer interface) has a shorter lifetime or a faster rate in returning to the closed channel state from which the receptor enters the desensitized state with an apparent faster rate as well. In other words, a shift of the channel opening equilibrium constant in the activation pathway (i.e., the same k_{op} but a larger k_{cl}), resulting in a higher concentration of the closed channel state, the on-the-pathway intermediate, consequently promotes a kinetically favorable desensitization pathway. This is equivalent to a rapidly interconverting system between the closed and open channel state that is being slowly converted to the desensitized state. Since the desensitization involves domain interface disengagement, such a domain rupture prevents the cleft closure from opening the channel (*37*). In the context of this structural framework, the channel closing rate process is kinetically linked to the channel desensitization rate process, via the closed channel state. In the step of channel closing from the open to the closed channel state, the dimer interface remains intact, whereas in the step of channel desensitization from the closed channel to the desensitized state, the dimer interface ruptures. In this sequence of events, the alternative splicing in GluR2 does influence the channel desensitization, but it does so by affecting the channel closing rate.

Although the magnitude of k_{cl} is used here to infer the role of the flip/flop sequence cassette in stabilizing the dimer interface and in turn in influencing the rate of channel desensitization, it should be emphasized that because k_{cl} is not a structural parameter, an interpretation of the difference in k_{cl} values between two receptors and/or two receptor isoforms, as in this case, is independent of any structural information. In fact, the hypothesis we put forth, i.e., linking the channel closing to channel desensitization via the closed channel state, based on our results from the intact receptors, is a general one in that if proven correct, it predicts that any mutation made anywhere, not necessarily just at the interface, would affect channel desensitization if the mutation affects the channel closing rate or the stability of the open channel conformation. One such mutant is GluR2 R628E whose rate of desensitization is found to be slower than that of wild-type GluR2 (*45*). Furthermore, R628 is not at the dimer interface or within the ligand binding domain (*45*). Therefore, the rapid kinetic study of this mutant in the future to determine the effect of this mutation on k_{cl} would provide a test of our hypothesis.

Alternative Splicing and GluR1 Receptor Channel Opening. We now examine the effect of the alternative splicing of the GluR1 receptor subunit on the channel opening and channel desensitization rate processes. According to our model described above, if two channels or two receptor isoforms have an identical rate constant of channel closing, then the channel desensitization rate constant is supposed to be the same. This is exactly what was observed for the flip and flop isoforms of GluR1: both had k_{cl} values of the same magnitude (Figure 5B and Table 3), and they also desensitized with the same rate at a given glutamate concentration (Figure 3B).

Unlike GluR2 and GluR3 (*13*), the flip/flop sequence cassette of GluR1 did not produce two kinetically different isoforms to influence the rate of channel closing. The alternative splicing in GluR1 had neither an effect on the free energy of the transition state nor an effect on the open channel state (see the legend of Figure 6). As far as its gating properties are concerned, GluR1 could be an "outlier" of the AMPA receptors. GluR2, GluR3, and GluR4 are kinetically similar to each other (*13, 18, 19*), but different from GluR1 (*17*), based on a systematic kinetic characterization of channel opening properties for all of the AMPA receptor subunits. For instance, any of the k_{op} values in GluR 2−4 is at least 3-fold larger than the value of k_{op} of GluR1; the K_1 and EC_{50} values of GluR2−4 are all ≥1 mM (*11, 18, 19*), whereas the corresponding value of GluR1 is ~0.5 mM (*17*). Furthermore, only the flip/flop pair in GluR1 does not exhibit different rates of desensitization (*6, 12, 23*), nor does the pair show a difference in the rate of channel closing as we now find from this study. We speculate that a lack of ability to regulate the channel closing rate process and thus the rate

of channel desensitization in GluR1 is due to its specific amino acid sequence in the flip/flop cassette. An earlier study of the alternative splicing in GluR1 (*23*) showed that mutations at Ser750 in $GluR1_{flip}$, which is within the flip/flop sequence cassette, can actually lead to different desensitization rate constants at a given glutamate concentration. This result therefore demonstrates that a critical amino acid position located in the alternatively spliced region is capable of modifying the channel properties. Furthermore, kinetic measurement and model fitting of differential effects of aniracetam and cyclothiazide, two AMPA receptor modulators, on the channel desensitization of the Ser750 mutants also suggested that these compounds may exert their effects on channel desensitization by slowing the channel closing rate process (*23, 30*).

The results from this study also raise new questions that await further investigations. For instance, it is not clear whether the magnitude of k_{cl} is linearly correlated to the magnitude of the channel desensitization rate constant. More studies are needed to clarify this question. Another question is whether the specific flip/flop sequence of GluR1 is the cause of its inability to control the channel-closing process. One possible experiment to address this question is to replace the flip/flop sequence of GluR1 with that of GluR2; if true, the GluR2 flip sequence-containing GluR1 should show a difference in k_{cl} and correspondingly in the rate of channel desensitization from either the wild-type GluR1 or the GluR2 flop sequence-containing GluR1. Furthermore, a modeling study of G1uR1, for instance, further predicts that three successive glycine residues in the flip/flop sequence region confer a structural flexibility which may result in functional differences between the flip and flop variants (*46*).

Implication of Alternative Splicing in AMPA Receptor Function. The results from this study have revealed that the alternative splicing regulates the channel opening kinetic properties of GluR2 and GluR3, but not those of GluR1. Given that the flip/flop sequence cassette affects channel opening kinetics, but only by affecting how fast an open channel closes, it is expected that the alternative splicing exerts its functional influence on channel activities only at low glutamate concentrations. This can be illustrated by the reduction of eq 1 to $k_{obs} \approx k_{cl}$, when the agonist concentration becomes low (or $L \ll K_1$). Consequently, the functional influence of alternative splicing for GluR2, for instance, can be manifested by the time course of channel opening with low glutamate concentrations. Under such a condition, as seen in eq 1, it is the k_{cl}, rather than the k_{op}, that dominates the channel opening kinetics. However, when the agonist concentration is high or $L > K_1$, the k_{op} will begin to dominate the time course. Because of identical k_{op} values for both the flip and flop isoforms of either GluR2 or GluR3 and because $k_{op} \gg k_{cl}$, the channel opening kinetic process between the flip/flop pair is virtually unaffected. Thus, any functional role that alternative splicing may play would become insignificant when glutamate concentrations are high. Furthermore, when glutamate concentration becomes low enough so that the ligand binding reaction becomes dominant, then the time course of the macroscopic current will no longer be reflective of the channel closing rate process.

A number of glutamatergic activities are associated with low glutamate concentrations, involving low AMPA channel activities, such as the slow-rising component of the AMPA receptor-mediated conductance at the cerebellar mossy fiber-granule cell synapse (*47*). In this case, a slow synaptic current is mediated possibly by two mechanisms, a slow local release of glutamate through a narrow fusion pore or glutamate spillover from distant sites (*47*). Both mechanisms may involve a low synaptic glutamate concentration. For example, in the cerebellar mossy fiber-granule cell synapse, a glutamate concentration of ~130 μM through a spillover mechanism is thought to be responsible for the slow-rising EPSC (*47*). This glutamate concentration would correspond to roughly 6% of the channel population being in the open channel state or the kinetic process of the channel activity reflecting essentially the k_{cl} component (see eq 1). As such, the kinetically distinct flip and flop variants may be relevant for synaptic transmission for GluR2 and GluR3, but not for GluR1. Furthermore, both spillover and narrow fusion pore release are thought to play important roles in the developmental strengthening of central glutamatergic synaptic connections (*47, 48*). Obviously, this conclusion is drawn from the kinetic property of individual subunits. However, because GluR2 and GluR3 are similar in this regard, the heteromeric assembly of these two subunits may behave the same. It is also possible that the receptor isoform dominates the behavior of the receptor complex. For instance, a rapid desensitization is observed with the medial nucleus of the trapezoid body relay neurons which most likely express only flop isoforms of GluR1, GluR2, and GluR4 (*10*). Interestingly, an assembly of the GluR2 flip variant with other AMPA receptor subunits, irrespective of the flip and flop status of the latter receptors, reduces the desensitization rate of the heteromeric receptor, as compared with the homomeric channel (*6*).

Abnormal expression of the flip and flop isoforms has been observed in some neurological diseases (*49*−*52*). In the spinal motor neurons of patients with amyotrophic lateral sclerosis (ALS), for instance, the level of the AMPA receptor flip variants is significantly elevated relative to that of the flop variants (*52*). Such an increase in the level of flip isoform expression in fact renders those neurons more vulnerable to glutamate insult (*52, 53*), since the flip isoforms close their open channels relatively more slowly and also desensitize relatively more slowly, as compared with the flop variants. Consequently, more calcium can enter the cell. Therefore, developing isoform-selective inhibitors as drug candidates may be a meaningful strategy in drug design.

Alternative splicing is an important mechanism in generating proteomic diversity and in modulating protein activities in a temporal and spatial manner (*54, 55*). The difference in the kinetic properties of AMPA receptors as illustrated in this study is a demonstration of the functional diversity conferred on the sequence subject to alternative splicing. Therefore, the alternative splicing in the extracellular ligand binding domain that gives rise to the flip and flop variants is a naturally built-in structural determinant for regulating the channel activity over the entire time course of ligand−receptor interaction: the alternative splicing regulates the rate of channel closing or the lifetime of the open channel state in the microsecond time domain, and in the millisecond time scale, it continues to regulate the rate of channel desensitization.

ACKNOWLEDGMENT

We are grateful to Steve Heinemann for the $GluR1_{flop}$ and $GluR2Q_{flop}$ clones and Mark Flex for helpful discussion.

REFERENCES

1. Sommer, B., Keinanen, K., Verdoorn, T. A., Wisden, W., Burnashev, N., Herb, A., Kohler, M., Takagi, T., Sakmann, B., and Seeburg, P. H. (1990) Flip and flop: A cell-specific functional switch in glutamate-operated channels of the CNS. *Science 249*, 1580–1585.
2. Rogers, S. W., Hughes, T. E., Hollmann, M., Gasic, G. P., Deneris, E. S., and Heinemann, S. (1991) The characterization and localization of the glutamate receptor subunit GluR1 in the rat brain. *J. Neurosci. 11*, 2713–2724.
3. Hollmann, M., and Heinemann, S. (1994) Cloned glutamate receptors. *Annu. Rev. Neurosci. 17*, 31–108.
4. Jonas, P., and Sakmann, B. (1992) Glutamate receptor channels in isolated patches from CA1 and CA3 pyramidal cells of rat hippocampal slices. *J. Physiol. 455*, 143–171.
5. Erreger, K., Chen, P. E., Wyllie, D. J., and Traynelis, S. F. (2004) Glutamate receptor gating. *Crit. Rev. Neurobiol. 16*, 187–224.
6. Mosbacher, J., Schoepfer, R., Monyer, H., Burnashev, N., Seeburg, P. H., and Ruppersberg, J. P. (1994) A molecular determinant for submillisecond desensitization in glutamate receptors. *Science 266*, 1059–1062.
7. Fleck, M. W., Bahring, R., Patneau, D. K., and Mayer, M. L. (1996) AMPA receptor heterogeneity in rat hippocampal neurons revealed by differential sensitivity to cyclothiazide. *J. Neurophysiol. 75*, 2322–2333.
8. Lambolez, B., Ropert, N., Perrais, D., Rossier, J., and Hestrin, S. (1996) Correlation between kinetics and RNA splicing of α-amino-3-hydroxy-5-methylisoxazole-4-propionic acid receptors in neocortical neurons. *Proc. Natl. Acad. Sci. U.S.A. 93*, 1797–1802.
9. Monyer, H., Seeburg, P. H., and Wisden, W. (1991) Glutamate-operated channels: Developmentally early and mature forms arise by alternative splicing. *Neuron 6*, 799–810.
10. Geiger, J. R., Melcher, T., Koh, D. S., Sakmann, B., Seeburg, P. H., Jonas, P., and Monyer, H. (1995) Relative abundance of subunit mRNAs determines gating and Ca^{2+} permeability of AMPA receptors in principal neurons and interneurons in rat CNS. *Neuron 15*, 193–204.
11. Koike, M., Tsukada, S., Tsuzuki, K., Kijima, H., and Ozawa, S. (2000) Regulation of kinetic properties of GluR2 AMPA receptor channels by alternative splicing. *J. Neurosci. 20*, 2166–2174.
12. Quirk, J. C., Siuda, E. R., and Nisenbaum, E. S. (2004) Molecular determinants responsible for differences in desensitization kinetics of AMPA receptor splice variants. *J. Neurosci. 24*, 11416–11420.
13. Pei, W., Huang, Z., and Niu, L. (2007) GluR3 flip and flop: Differences in channel opening kinetics. *Biochemistry 46*, 2027–2036.
14. Wieboldt, R., Gee, K. R., Niu, L., Ramesh, D., Carpenter, B. K., and Hess, G. P. (1994) Photolabile precursors of glutamate: Synthesis, photochemical properties, and activation of glutamate receptors on a microsecond time scale. *Proc. Natl. Acad. Sci. U.S.A. 91*, 8752–8756.
15. Stern-Bach, Y., Russo, S., Neuman, M., and Rosenmund, C. (1998) A point mutation in the glutamate binding site blocks desensitization of AMPA receptors. *Neuron 21*, 907–918.
16. Pei, W., Ritz, M., McCarthy, M., Huang, Z., and Niu, L. (2007) Receptor occupancy and channel-opening kinetics: A study of GluR1 L497Y AMPA receptor. *J. Biol. Chem. 282*, 22731–22736.
17. Li, G., and Niu, L. (2004) How fast does the $GluR1Q_{flip}$ channel open? *J. Biol. Chem. 279*, 3990–3997.
18. Li, G., Pei, W., and Niu, L. (2003) Channel-opening kinetics of GluR2Q(flip) AMPA receptor: A laser-pulse photolysis study. *Biochemistry 42*, 12358–12366.
19. Li, G., Sheng, Z., Huang, Z., and Niu, L. (2005) Kinetic mechanism of channel opening of the $GluRD_{flip}$ AMPA receptor. *Biochemistry 44*, 5835–5841.
20. Pandit, A. D., Krantz, B. A., Dothager, R. S., and Sosnick, T. R. (2007) Characterizing protein folding transition States using Psi-analysis. *Methods Mol. Biol. 350*, 83–104.
21. Fersht, A. R. (2004) Phi value versus psi analysis. *Proc. Natl. Acad. Sci. U.S.A. 101*, 17327–17328.
22. Fersht, A. R., and Sato, S. (2004) Phi-value analysis and the nature of protein-folding transition states. *Proc. Natl. Acad. Sci. U.S.A. 101*, 7976–7981.
23. Partin, K. M., Fleck, M. W., and Mayer, M. L. (1996) AMPA receptor flip/flop mutants affecting deactivation, desensitization, and modulation by cyclothiazide, aniracetam, and thiocyanate. *J. Neurosci. 16*, 6634–6647.
24. Loftfield, R. B., and Eigner, E. A. (1969) Molecular order of participation of inhibitors (or activators) in biological systems. *Science 164*, 305–308.
25. Derkach, V., Barria, A., and Soderling, T. R. (1999) Ca^{2+}/calmodulin-kinase II enhances channel conductance of α-amino-3-hydroxy-5-methyl-4-isoxazolepropionate type glutamate receptors. *Proc. Natl. Acad. Sci. U.S.A. 96*, 3269–3274.
26. Wahl, P., Anker, C., Traynelis, S. F., Egebjerg, J., Rasmussen, J. S., Krogsgaard-Larsen, P., and Madsen, U. (1998) Antagonist properties of a phosphono isoxazole amino acid at glutamate R1−4 (R,S)-2-amino-3-(3-hydroxy-5-methyl-4-isoxazolyl)propionic acid receptor subtypes. *Mol. Pharmacol. 53*, 590–596.
27. Jin, R., Banke, T. G., Mayer, M. L., Traynelis, S. F., and Gouaux, E. (2003) Structural basis for partial agonist action at ionotropic glutamate receptors. *Nat. Neurosci. 6*, 803–810.
28. Heckmann, M., Bufler, J., Franke, C., and Dudel, J. (1996) Kinetics of homomeric GluR6 glutamate receptor channels. *Biophys. J. 71*, 1743–1750.
29. Raman, I. M., and Trussell, L. O. (1995) The mechanism of α-amino-3-hydroxy-5-methyl-4-isoxazolepropionate receptor desensitization after removal of glutamate. *Biophys. J. 68*, 137–146.
30. Vyklicky, L., Jr., Patneau, D. K., and Mayer, M. L. (1991) Modulation of excitatory synaptic transmission by drugs that reduce desensitization at AMPA/kainate receptors. *Neuron 7*, 971–984.
31. Rosenmund, C., Stern-Bach, Y., and Stevens, C. F. (1998) The tetrameric structure of a glutamate receptor channel. *Science 280*, 1596–1599.
32. Clements, J. D., Feltz, A., Sahara, Y., and Westbrook, G. L. (1998) Activation kinetics of AMPA receptor channels reveal the number of functional agonist binding sites. *J. Neurosci. 18*, 119–127.
33. Robert, A., and Howe, J. R. (2003) How AMPA receptor desensitization depends on receptor occupancy. *J. Neurosci. 23*, 847–858.
34. Cymes, G. D., Grosman, C., and Auerbach, A. (2002) Structure of the transition state of gating in the acetylcholine receptor channel pore: A phi-value analysis. *Biochemistry 41*, 5548–5555.
35. Armstrong, N., and Gouaux, E. (2000) Mechanisms for activation and antagonism of an AMPA-sensitive glutamate receptor: Crystal structures of the GluR2 ligand binding core. *Neuron 28*, 165–181.
36. Hansen, K. B., Yuan, H., and Traynelis, S. F. (2007) Structural aspects of AMPA receptor activation, desensitization and deactivation. *Curr. Opin. Neurobiol. 17*, 281–288.
37. Sun, Y., Olson, R., Horning, M., Armstrong, N., Mayer, M., and Gouaux, E. (2002) Mechanism of glutamate receptor desensitization. *Nature 417*, 245–253.
38. Horning, M. S., and Mayer, M. L. (2004) Regulation of AMPA receptor gating by ligand binding core dimers. *Neuron 41*, 379–388.
39. Armstrong, N., Jasti, J., Beich-Frandsen, M., and Gouaux, E. (2006) Measurement of conformational changes accompanying desensitization in an ionotropic glutamate receptor. *Cell 127*, 85–97.
40. Trussell, L. O., Thio, L. L., Zorumski, C. F., and Fischbach, G. D. (1988) Rapid desensitization of glutamate receptors in vertebrate central neurons. *Proc. Natl. Acad. Sci. U.S.A. 85*, 4562–4566.
41. Colquhoun, D., Jonas, P., and Sakmann, B. (1992) Action of brief pulses of glutamate on AMPA/kainate receptors in patches from different neurones of rat hippocampal slices. *J. Physiol. 458*, 261–287.
42. Tang, C. M., Dichter, M., and Morad, M. (1989) Quisqualate activates a rapidly inactivating high conductance ionic channel in hippocampal neurons. *Science 243*, 1474–1477.
43. Robert, A., Irizarry, S. N., Hughes, T. E., and Howe, J. R. (2001) Subunit interactions and AMPA receptor desensitization. *J. Neurosci. 21*, 5574–5586.

44. Robert, A., Armstrong, N., Gouaux, J. E., and Howe, J. R. (2005) AMPA receptor binding cleft mutations that alter affinity, efficacy, and recovery from desensitization. *J. Neurosci. 25*, 3752–3762.
45. Yelshansky, M. V., Sobolevsky, A. I., Jatzke, C., and Wollmuth, L. P. (2004) Block of AMPA receptor desensitization by a point mutation outside the ligand-binding domain. *J. Neurosci. 24*, 4728–4736.
46. Sutcliffe, M. J., Wo, Z. G., and Oswald, R. E. (1996) Three-dimensional models of non-NMDA glutamate receptors. *Biophys. J. 70*, 1575–1589.
47. Nielsen, T. A., DiGregorio, D. A., and Silver, R. A. (2004) Modulation of glutamate mobility reveals the mechanism underlying slow-rising AMPAR EPSCs and the diffusion coefficient in the synaptic cleft. *Neuron 42*, 757–771.
48. Renger, J. J., Egles, C., and Liu, G. (2001) A developmental switch in neurotransmitter flux enhances synaptic efficacy by affecting AMPA receptor activation. *Neuron 29*, 469–484.
49. Eastwood, S. L., Burnet, P. W., and Harrison, P. J. (1997) GluR2 glutamate receptor subunit flip and flop isoforms are decreased in the hippocampal formation in schizophrenia: A reverse transcriptase-polymerase chain reaction (RT-PCR) study. *Brain Res. Mol. Brain Res. 44*, 92–98.
50. Stine, C. D., Lu, W., and Wolf, M. E. (2001) Expression of AMPA receptor flip and flop mRNAs in the nucleus accumbens and prefrontal cortex after neonatal ventral hippocampal lesions. *Neuropsychopharmacology 24*, 253–266.
51. Seifert, G., Schroder, W., Hinterkeuser, S., Schumacher, T., Schramm, J., and Steinhauser, C. (2002) Changes in flip/flop splicing of astroglial AMPA receptors in human temporal lobe epilepsy. *Epilepsia 43*, 162–167.
52. Tomiyama, M., Rodriguez-Puertas, R., Cortes, R., Pazos, A., Palacios, J. M., and Mengod, G. (2002) Flip and flop splice variants of AMPA receptor subunits in the spinal cord of amyotrophic lateral sclerosis. *Synapse 45*, 245–249.
53. Kawahara, Y., Ito, K., Sun, H., Aizawa, H., Kanazawa, I., and Kwak, S. (2004) Glutamate receptors: RNA editing and death of motor neurons. *Nature 427*, 801.
54. Grabowski, P. J., and Black, D. L. (2001) Alternative RNA splicing in the nervous system. *Prog. Neurobiol. 65*, 289–308.
55. House, A. E., and Lynch, K. W. (2008) Regulation of alternative splicing: More than just the ABCs. *J. Biol. Chem. 283*, 1217–1221.

BI8015907